



**Shock Loading of IFE Target Chamber
Structures Study: Final Report for Contract
Number DE-FG02-97ER54413**

**Mark Anderson, Bhalchandra Puranik, Jason Oakley,
Paul Brooks, Robert Peterson, Riccardo Bonazza**

December 1998

UWFDM-1089

FUSION TECHNOLOGY INSTITUTE

UNIVERSITY OF WISCONSIN

MADISON WISCONSIN

DISCLAIMER

This report was prepared as an account of work sponsored by an agency of the United States Government. Neither the United States Government, nor any agency thereof, nor any of their employees, makes any warranty, express or implied, or assumes any legal liability or responsibility for the accuracy, completeness, or usefulness of any information, apparatus, product, or process disclosed, or represents that its use would not infringe privately owned rights. Reference herein to any specific commercial product, process, or service by trade name, trademark, manufacturer, or otherwise, does not necessarily constitute or imply its endorsement, recommendation, or favoring by the United States Government or any agency thereof. The views and opinions of authors expressed herein do not necessarily state or reflect those of the United States Government or any agency thereof.

**Shock Loading of IFE Target Chamber Structures Study:
Final Report for Contract Number DE-FG02-97ER54413**

Mark Anderson, Bhalchandra Puranik, Jason Oakley,
Paul Brooks, Robert Peterson, Riccardo Bonazza

Fusion Technology Institute
University of Wisconsin-Madison
1500 Engineering Drive
Madison, WI 53706

December 1998

UWFDM-1089

1. INTRODUCTION

A hydrodynamic issue in ICF (Inertial Confinement Fusion) that is suitable numerically and experimentally for study within a shock-tube is the removal of energy and protection of the first structural wall in future designs of reactors. Recent studies concerning the protection of the first structural wall of the reactor have been conducted leading to the proposal of INPORT (INHibited Flow in PORous Tube) and rigid PERIT (PERforated RIGid Tube) units (Kulcinski et al., 1994; see Figs. 1, 2). These units are hollow tubes which carry a PbLi eutectic alloy. The INPORT tubes are constructed out of a porous orthogonal weave of SiC, C, or steel which allows an ablative film of the PbLi to form on the outer surface of the tube which absorbs X-rays and target debris while the bulk of the liquid flowing through the tube absorbs the energy and mitigates the isochoric heating by the neutrons. The first few levels of the PERIT cooling arrangement have fan sprays, creating a liquid sheet of PbLi which performs essentially the same task as the film on the INPORT tube design. These tubes must be able to withstand the high impact and diffraction of the shock-wave formed by the thermonuclear reaction of the DT (deuterium and tritium) fuel. To determine the pressure load and distribution, which is needed to determine the acceleration and vibration of the tubes, it is possible to conduct shock diffraction studies within a shock-tube. Bryson and Gross (1960), and Syshchicova et al. (1967), conducted some initial studies recording the shock formations at different times after an initial shock-cylinder interaction. This information is quite valuable; however, only the formation and geometrical aspects of the reflected and diffracted shocks were investigated while the pressure distribution around the cylinder was not studied. The British Atomic Weapons Research Establishment (Bishop and Rowe, 1967) added to this experimental data and was able to measure the pressure distribution on a cylinder in a blast channel with piezoelectric pressure transducers; however, due to the limitations of the blast channel, only experiments with low Mach numbers were conducted. Recently, the need for experimental pressure data to compare with numerical solutions, and the lack of a robust facility for directly measuring pressures at high Mach numbers, have prompted several studies using holographic interferometry (Heilig, 1969). This method works well and an estimate of the pressure distribution can be made from the experiments using the density gradients and an assumed equation of state. Although these types of measurements are helpful for comparing with computer simulations, they are not direct measurements of the pressure distribution and it is difficult to calculate the initial acceleration and force due to the shock-wave from them. In an effort to increase the extent of the experimental database, pressure distributions for strong shocks are directly measured in a large, square inner cross section shock-tube capable of achieving Mach numbers on the order of 5 into atmospheric air and considerably higher into vacuum. The time history of the pressure distribution is recorded with piezoelectric pressure transducers mounted flush on a cylindrical surface. Numerical investigations of the experiment are conducted to obtain more quantitative data, such as the density and pressure of the flow field.

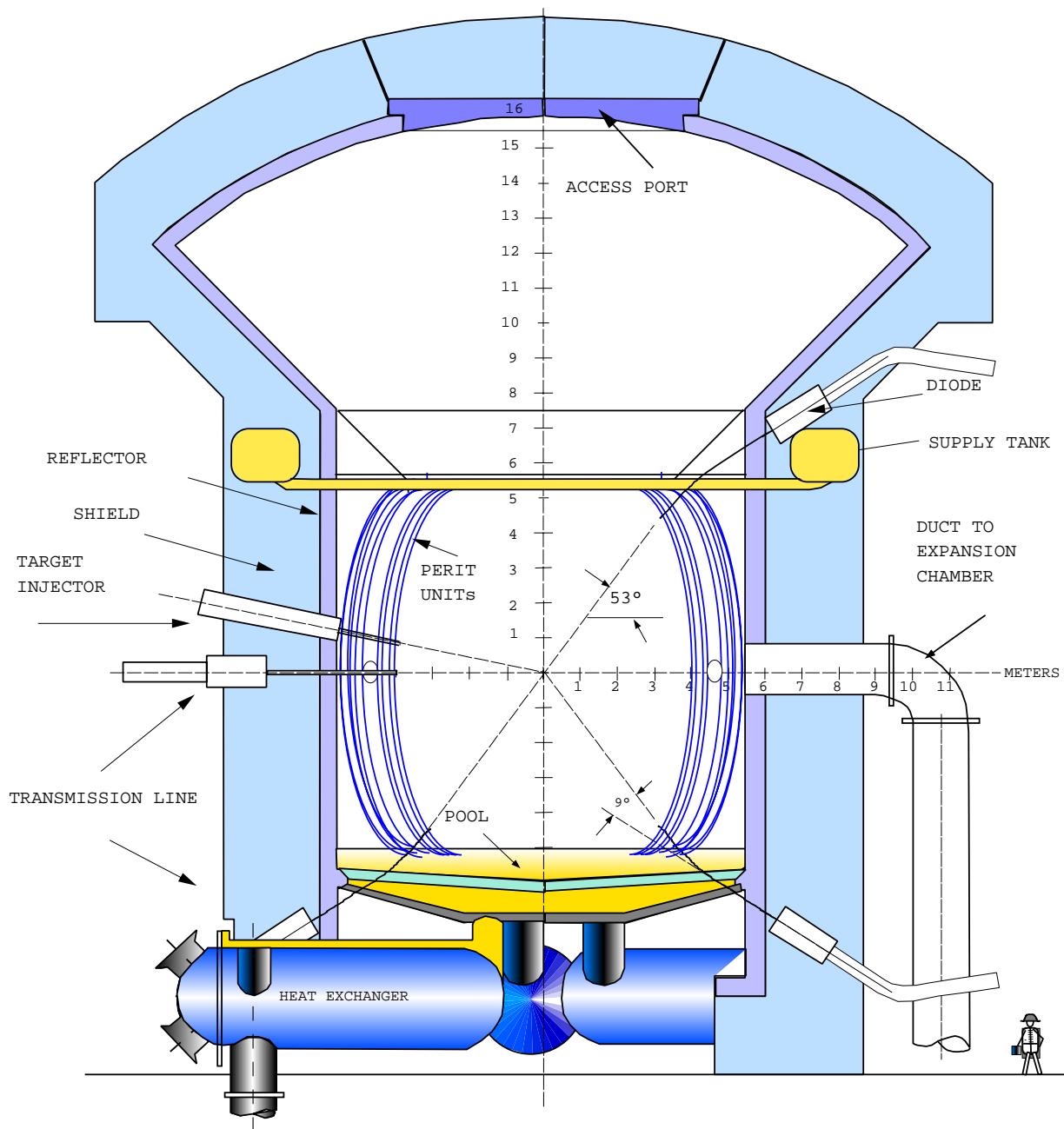


Figure 1. LIBRA reactor. Shown are the PERIT tubes used to remove the energy and protect the structural wall of the reactor after an explosion from the DT pellet in the center of the reactor. A fan spray from the first few levels of the PERIT tubes would create a liquid PbLi sheet (schematic taken from Kulcinski et al. (1994)).

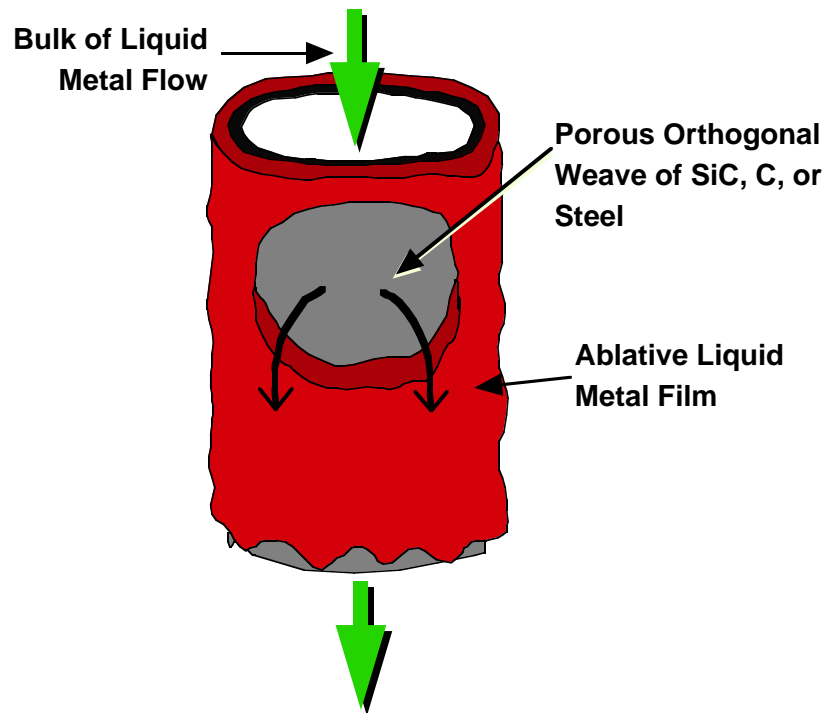


Figure 2. Design of the INPORT tubes. PbLi flows through the tube and forms an ablative liquid layer by flowing through a porous weave of SiC, C or steel (schematic taken from Kulcinski et al. (1994)).

2. EXPERIMENTAL FACILITY

2.1. The Wisconsin Shock-Tube

A new shock-tube (WIStube) has been fabricated for the study of the shock-cylinder interactions (Fig. 3). The tube is vertical, with a large square inner cross section ($25\text{ cm} \times 25\text{ cm}$) and is 9.2 m long. The square cross section provides the parallel walls necessary for flow visualization without resorting to a structurally weak tube extension (Meshkov, 1969). It has a structural capability to withstand a 20 MPa pressure load. Thus, strong shocks can be fired into a driven section initially at atmospheric pressure. The driven section can also be evacuated resulting in extremely large Mach number shocks approaching the strengths anticipated in future IFE (Inertial Fusion Energy) devices. The driver section is made from a circular, chrome-plated carbon steel pipe, 46 cm OD, 1.9 cm thick and 2 m long. It is equipped with four ignition tubes mounted inside the driver section, capable of igniting a stoichiometric mixture of oxygen and hydrogen diluted in helium to produce high pressure and temperature driver conditions. To release the shock into the driven section, a metal diaphragm is ruptured either by pressurizing the driver section using compressed gas bottles or, when the hydrogen-oxygen combustion approach is used, by detonation of an explosive charge placed around the circumference of the diaphragm. Sharp knife edges, in the form of a cross, are placed just below the diaphragm to facilitate its rupture in the form of four petals. After the diaphragm is ruptured, the four petals remain attached to the diaphragm along its circumference. Table 1 lists the diaphragm material, the

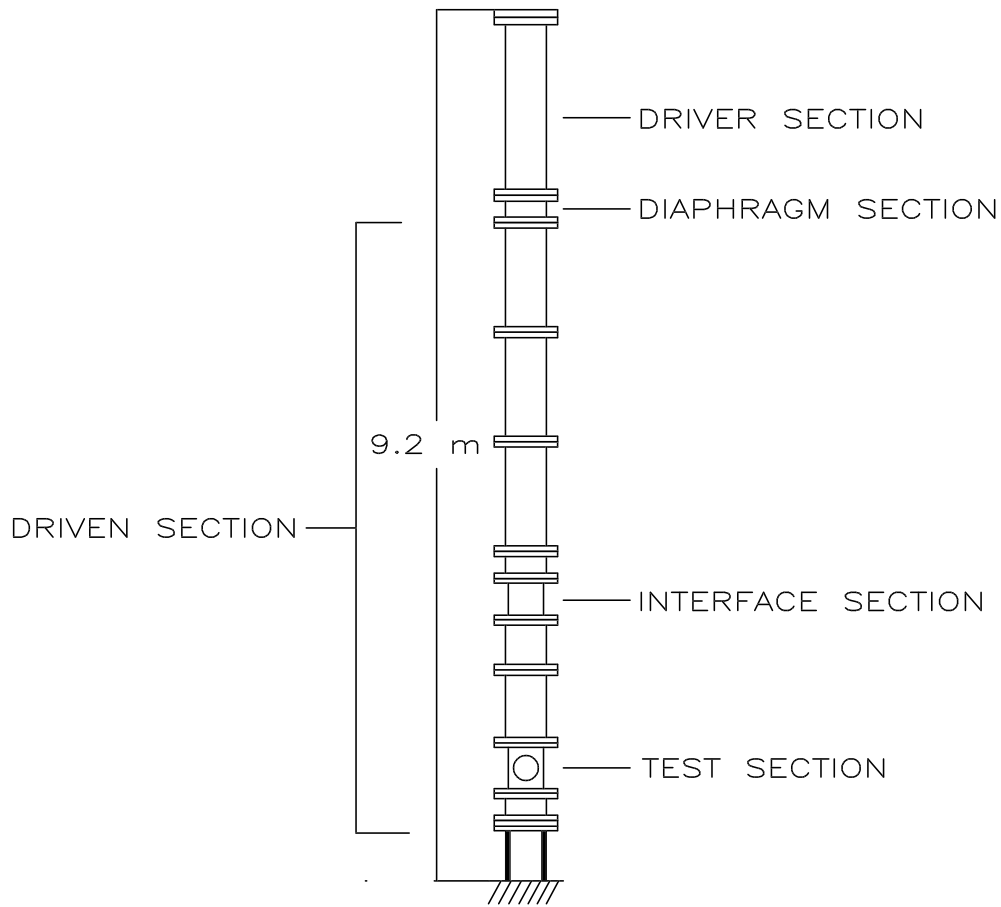


Figure 3. Schematic of the primary features of the shock-tube. The shock-wave is created by high pressure gas in the driver section, rupturing a diaphragm. The shock-wave travels down the tube and interacts with the cooling tube model.

diaphragm thickness, the driver gas and the Mach number of the shock-wave generated upon rupturing it. The repeatability of the shock strength is confirmed to within $\pm 0.4\%$.

Figure 4 shows the cross section of the driven section. An internal liner, consisting of four stainless steel plates 1 cm thick, welded together, is supported by a concrete matrix contained in a circular carbon steel pipe, 46 cm OD to form a segment of the driven section. These segments are then capped with a class 300# A-105 flange welded to the top and bottom of the tube. This allows any of the nine sections that make up the tube, to be bolted together.

The test section consists of four steel plates, chrome plated on their inside surface, 7 cm thick, welded together to form a box with a 25.4 cm square inside cross section. The test section contains two circular ports 28 cm in diameter, on opposite sides. Fused quartz windows, 24 cm in diameter and 9 cm thick, are mounted in these ports for optical access.

Material	Description	Rupture Pressure (psia)	Driver Gas	Mach Number
Al 5052	One sheet, 0.015" thick	33	Air	1.25
Al 5052	Two sheets, 0.015" thick	39	Air	1.28
Al 5052	One sheet, 0.06" thick	136	Air	1.66
Steel A366	One sheet, 0.034" thick	217	Air	1.85
Al 5052	Two sheets, 0.06" thick	244	Air	1.86
Al 5052	Four sheets, 0.06" thick	365	Air	2.00
Steel A366	One sheet, 0.055" thick	365	Air	2.00
Steel A366	Two sheets, 0.055" thick	565	Air	2.15
Steel A366	Three sheets, 0.055" thick	661	Air	2.23
Steel A366	One sheet, 0.1196" thick	750	Air	2.28
Steel A366	One sheet, 0.055" thick	372	He	2.77
Steel A366	Two sheets, 0.055" thick	550	He	3.08

Table 1. Diaphragm Characterization Data

The end wall of the shock-tube contains a circular, fused quartz window, 14 cm in diameter, 6 cm thick, centered 7.5 cm from the inner wall of the tube. A laser sheet can be projected upward at various distances from the centerline of the tube for planar imaging of the shocked cylinder.

2.2. Instrumentation

The driver section is equipped with a pressure gauge and a thermocouple to measure the pressure and the temperature of the driver gas just before the release of the shock. The driven section has pressure transducer ports at various locations along its length. Piezoelectric pressure transducers are mounted in these ports, flush with the inner wall of the tube, to measure the shock speed and trigger the flow diagnostics hardware. Both the driver and driven sections can be evacuated to 7 torr.

Since the velocities of the shock-wave are on the order of 1000 m/s or higher, imaging times on the order of tens of nanoseconds are required to obtain sharp images. In a first series of flow visualization experiments using the shadowgraph technique, either a modified Continuum (Surelite II-PIV) pulsed Nd:YAG laser or an arc discharge lamp is used as a light source for the imaging. The laser consists of two laser cavities capable of delivering 250 mJ/pulse (and hence 500 mJ/pulse when the beams are superimposed) at $\lambda=532$ nm. The pulse width is 10 ns, thus making it suitable for imaging such high speed flows. The Xenon Inc. Model-437B short duration 20 ns broad spectrum, arc discharge lamp is used in some experiments to attain a more spatially uniform collimated light source than can be achieved with the laser. A 16-bit CCD camera (Spectra Video Series, by Pixel Vision) is used to capture the flow field images. It has a back-lit, 1024×1024 pixel array, a thermo-electrically cooled sensor and a low speed (40 kHz) transfer rate that guarantees low dark current and readout noise ($1 e^-/\text{pix s}$ and $5-8 e^-$ rms respectively, @ -45° C). One image is obtained per event. An HP-Infinium 4 channel digital oscilloscope with

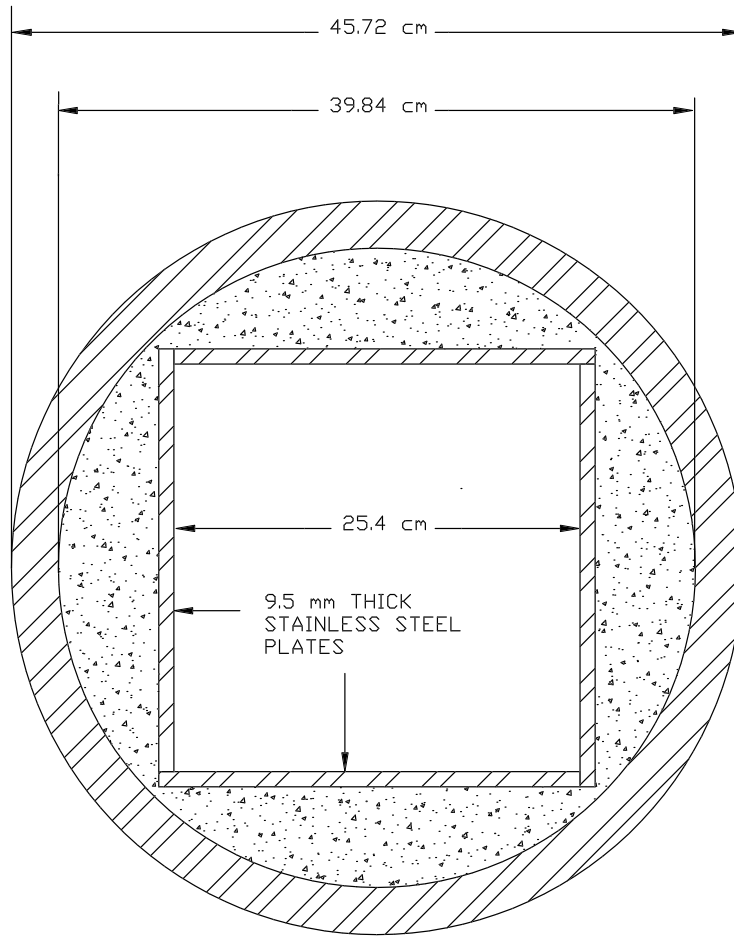


Figure 4. Details of tube construction; the outer circular cross section is steel with a stainless steel square cross section in the center. The volume between the outer steel tube and the inner wall is filled with concrete.

a sampling rate of 1 GHz per channel is used to record the pressure traces from the piezoelectric pressure transducers.

2.3. Diagnostics

Four wall-mounted pressure transducers are used in every experiment. The transducer closest to the diaphragm triggers the light source to pulse, through a variable delay box. The delay is set such that the laser pulses when the shock-wave is at the appropriate position in the test section, so that the temporal evolution of the flow field behind the shock and around the cylinder can be imaged. The delay is calculated from 1-D gas dynamics and previous experiments correlating the thickness of the diaphragm to shock speeds. The shock speed is measured from the traces obtained by two other wall mounted pressure transducers. The last pressure transducer is mounted in the end wall to measure the highest pressure generated behind the reflected shock.

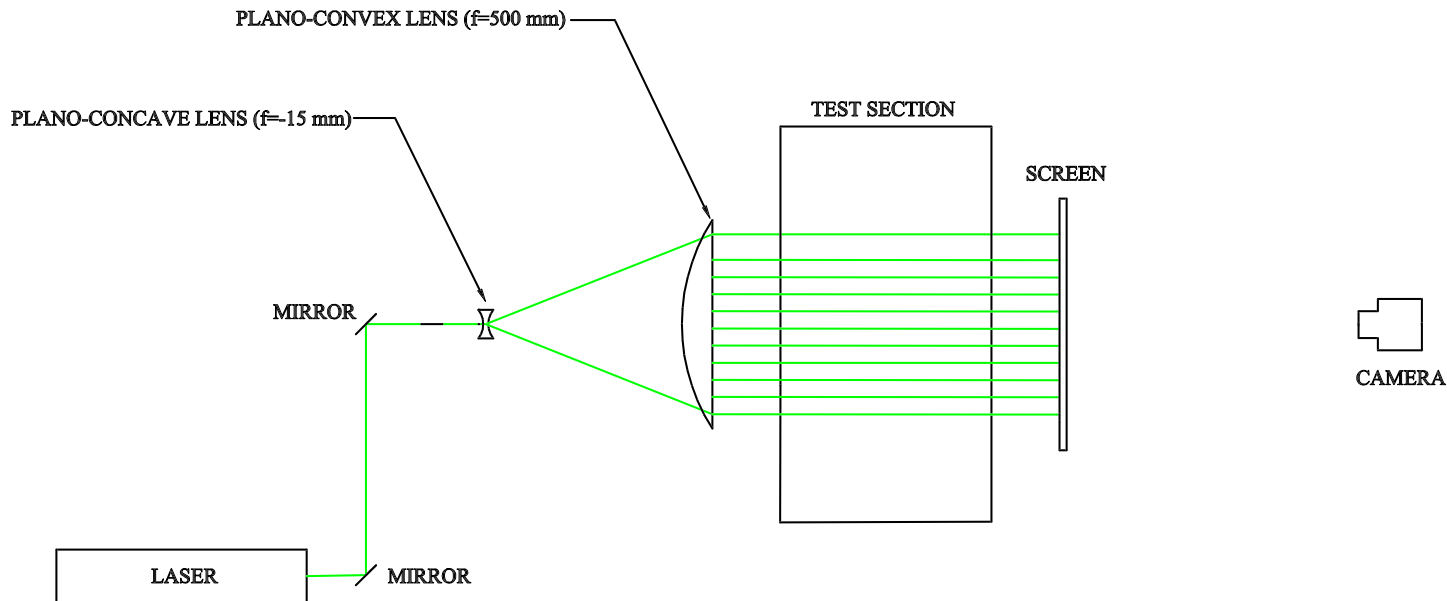


Figure 5. Optical setup for shadowgraph diagnostics. The viewing area in the test section is 21.6 cm; however, in the current setup the illuminating light source is only expanded to 14 cm. As the light rays pass through the test section they are deflected by changes in the density gradient creating a picture on the screen.

In addition to the pressure transducers that trigger the laser and measure the shock speed, four more are mounted on the cylinder at 0, 30, 60 and 90 degrees, as measured from the topmost point on the cylinder. There are also two accelerometers added to measure the vertical and horizontal acceleration of the cylinder due to the shock interaction. The specifics of the cooling tube modeling cylinder will be discussed in the next section.

A shadowgraph system is used to image the shock diffraction. Figure 5 shows the optical setup for the experiment. The laser beam is spatially filtered before it is expanded by a plano-concave lens (focal length -15 mm). It is then collimated by a plano-convex lens (focal length 375 mm) into a parallel beam of diameter 212 mm. The collimated beam is passed through the test section windows and projected on a screen. The CCD camera is focused on the screen and captures the light produced by either the laser or the arc discharge lamp.

At the time of an experiment, the whole optical setup and a portion of the shock-tube containing the test section are surrounded by an enclosure made from thick theater curtains so the area surrounding the test section is completely dark. The camera shutter is opened, and the CCD exposure is started prior to the rupture of the diaphragm (the diaphragm rupture pressure is known from the previous experiments). After the diaphragm is ruptured, the shock triggers

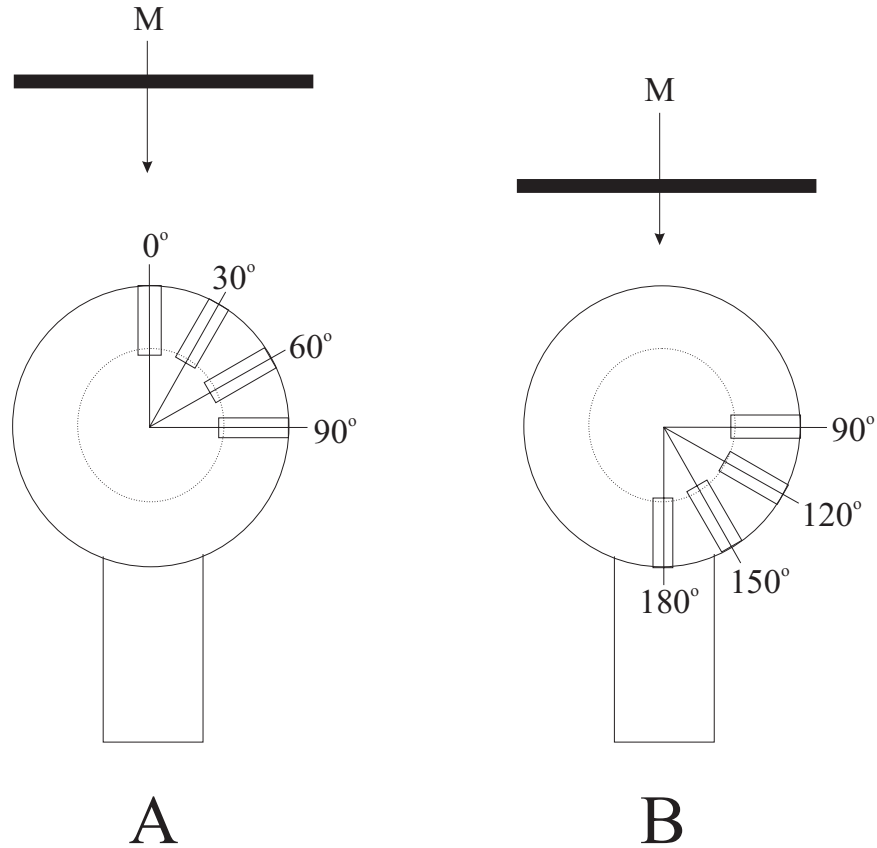


Figure 6. Schematic of the pressure transducer locations. The tube can be rotated 90° so the pressure distribution around the whole tube can be measured.

the diagnostics as described above and an image of the flow field of interest is obtained with the CCD camera.

3. PRELIMINARY RESULTS

Typical shock-tube data are presented for the ICF reactor cooling tube study. Data include pressure and accelerometer summaries and a time history of shadowgraph pictures depicting the diffraction of the shock-wave around the cylinder. Numerical simulations of the pressure, mass density, and velocity of the flow for these experiments have been performed and are in qualitative agreement with the shadowgraph photos.

3.1. Experimental Investigation

The cooling tubes in an ICF reactor are subject to repeated shocks from the ignition of DT fuel reactions that occur in rapid succession. For proper design, it is necessary to understand the force load history on the cooling tubes. The cooling tubes are long cylinders that have a slight

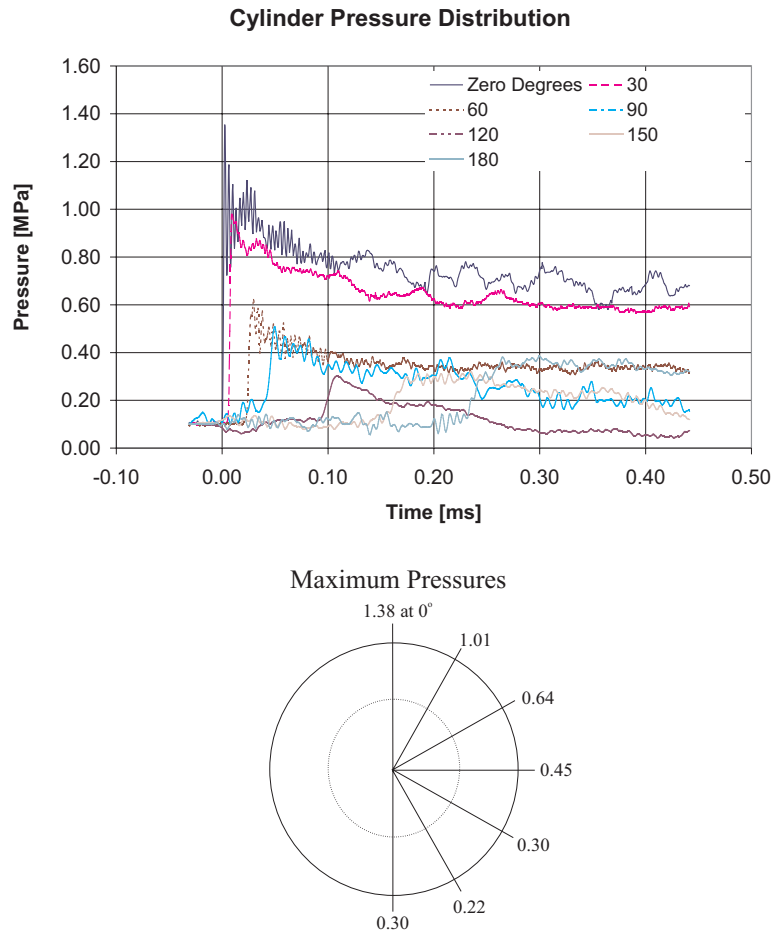


Figure 7. Pressure traces from the transducers located on the cylinder during shock diffraction. The separation in time indicates the relative position of the pressure transducers. The first trace is from the pressure transducer on the top of the cylinder. The lower figure shows the maximum pressure generated at the different measurement locations around the cylinder.

curvature along the azimuthal axis as shown in Fig. 1. The WIStube studies the shock-loading on an ICF cooling tube modeled with a 25.4 cm long cylinder, 3.175 cm in radius, placed in the center of the test section. The 25.4 cm length completely spans the 25.4 cm cross section of the tube and permits a two dimensional fluid dynamics study of shock-induced transient flow around a cylinder. Two 2.54 cm diameter fixed rods are in place at each end of the tube to vertically support it during the experiment. Accelerometers are mounted vertically and horizontally on the interior diameter (1.27 cm) of the cooling tube model. The hollow portion of the tube also serves as a cable-way for the transducers' cables. The piezoelectric shock pressure transducers are mounted as shown in Fig. 6. The surface of the pressure transducers are flush mounted with the surface of the cylinder. There are four pressure transducers mounted in the central region of the cylinder. For each Mach number, seven pressure histories are recorded. First, pressure histories are recorded at 0, 30, 60 and 90 degrees, as shown in Fig. 6A. Next, the model cooling cylinder is

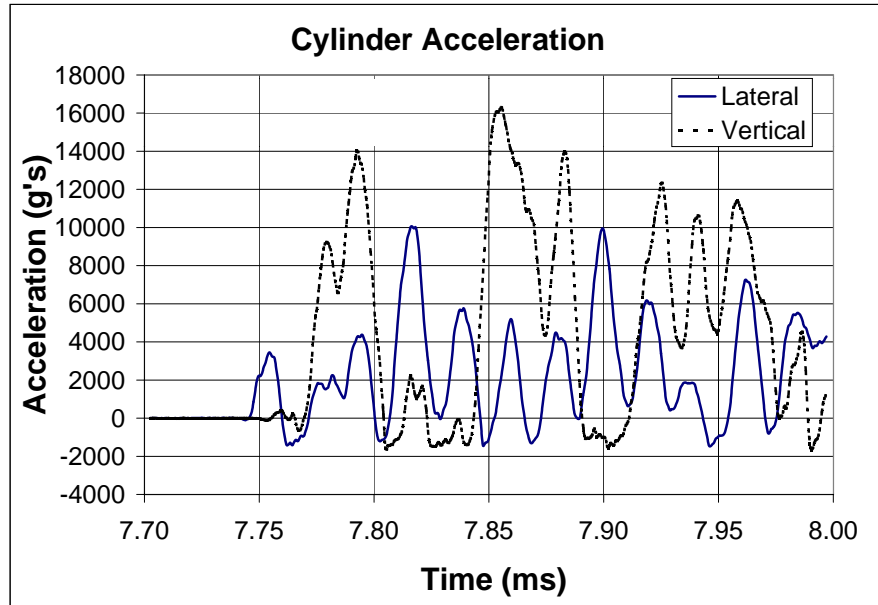


Figure 8. Vertical and horizontal acceleration of the cylinder during shock diffraction. The acceleration perpendicular to the shock is significantly higher than the lateral acceleration.

rotated 90 degrees and pressure histories are recorded at 90, 120, 150 and 180 degrees, as shown in Fig. 6B. Several experiments are conducted with the cylinder in each position so that statistically consistent measurements are made and, also, an adequate photographic shock history is obtained.

The presented data are for a Mach 1.85 shock in air at atmospheric pressure and temperature. The peak initial pressure and pressure history are shown in Fig. 7. The circular figure presents the maximum initial pressure distribution around the cylinder while the graph shows the time history of the pressure distribution. Qualitatively, the figure reveals that the maximum pressure occurs at the top of the cooling tube model (normal to the shock) and then decreases as the angle (relative to the upwards vertical) increases. For impulsive force measurements needed for cooling tube design, it is necessary to integrate the pressure history data for each angular segment of the cylinder as a function of time. The maximum pressure occurs “instantaneously” at the top of the tube; however, the force on the tube must be determined by integrating the seven pressure time series over the surface of the tube. The maximum vertical acceleration measured on the tube is 13,800 g 's. This result cannot be used directly because of differences between the cooling tube prototype and the cooling tube model, both in the size of the tube and the manner in which it is supported. However, numerical studies of the structural response of the tube model to impulsive loading are in progress and the results will be compared against the experimental data shown in Fig. 8. Upon such validation, the numerical model will represent a useful design tool for the final cooling tube prototype.

Visual diagnostics for these experiments use the shadowgraph technique, optically sensitive to the second derivative of the density gradient (Yang, 1989). Three shadowgraph results are

shown in Fig. 9. The thick black vertical structures between the cylinder and the bottom of each of the photographs are the two (inline) support rods. The optical diagnostic provides a history of the transmitted shock moving around the cylinder. The initial shock is planar (it appears as a horizontal dark line above the cylinder in Fig. 9a). A most significant feature of the three shadowgraph pictures shown in Fig. 9 is the bulbous shock reflection from the surface of the cylinder. The transmitted shock remains planar as it travels vertically downward (except where it is attached to the cylinder and a Mach stem is formed); however, the reflected shock off of the cylinder surface is curved (as expected). The radius of the reflected shock grows in time as the transmitted shock travels down the cylinder. The time series of photographs reveal the behavior of both the planar shock and gas flow around the cylinder.

The combination of dynamic pressure history, acceleration data and optical diagnostics provide a unique experimental characterization of the ICF cooling tube model when subjected to shock loading. This new experimental apparatus provides an important understanding of the structural response of the tube to shock-loading needed for the ICF cooling tube design.

3.2. Computer Simulations

Computer simulations of the above shock-tube experiments have been performed. One major goal of ICF experiments is to validate computer codes, and shock-tube experiments allow a unique database for this comparison. Two computer codes have been used in this effort: BUCKY (MacFarlane et al., 1995) and RAGE¹. BUCKY is used to model the propagation of the shock from the driver section, through the tube, and to a point just before the shock begins to interact with the cylinder inserted in the shock-tube. RAGE is used to simulate the interaction of the shock with the cylinder.

BUCKY is a 1-D Lagrangian radiation-hydrodynamics computer code developed at the University of Wisconsin-Madison. Equations-of-state and opacities are read from either SESAME (Bennett et al., 1978) tables from Los Alamos National Laboratory or tables produced by the University of Wisconsin EOSOPA (Wang, 1993). The calculated pressure, mass density and velocity profiles are shown in Figures 10, 11, and 12. At 9 ms after the diaphragm bursts, the shock reaches a position about 800 cm from the back of the driver section, which is 190 cm above the bottom of the tube. The cylinder is centered 57.864 cm above the bottom of the tube and has a radius of 3.175 cm. The mass density behind the shock at this point is about 3.5 mg/cm³, the pressure is 0.42 MPa and the velocity is 390 m/s.

RAGE is a 1, 2 or 3-D adaptive mesh refinement radiation-hydrodynamics computer code. It is being developed by SAIC and LANL. RAGE runs have used the BUCKY results at 9 ms mentioned above as initial conditions. The mass density at 11.50 ms is shown in Fig. 13. Here, the shock has moved partially around the cylinder and the rarefaction of the shock at the back side of the cylinder can begin to be seen. This is in qualitative agreement with the shadowgraph images shown in Fig. 9. A bug was discovered in RAGE when we attempted to do a quantitative comparison between RAGE and the measured pressures predicted in Fig. 7. LANL is repairing that bug and those comparisons will be made.

¹RAGE is a one, two, and three dimensional, multimaterial Eulerian hydrodynamics code developed by SAIC for use in solving a variety of high deformation flow of materials problems. The RAGE code manual is available on-line at <http://www-xdiv.lanl.gov/XTA/rageman/>.

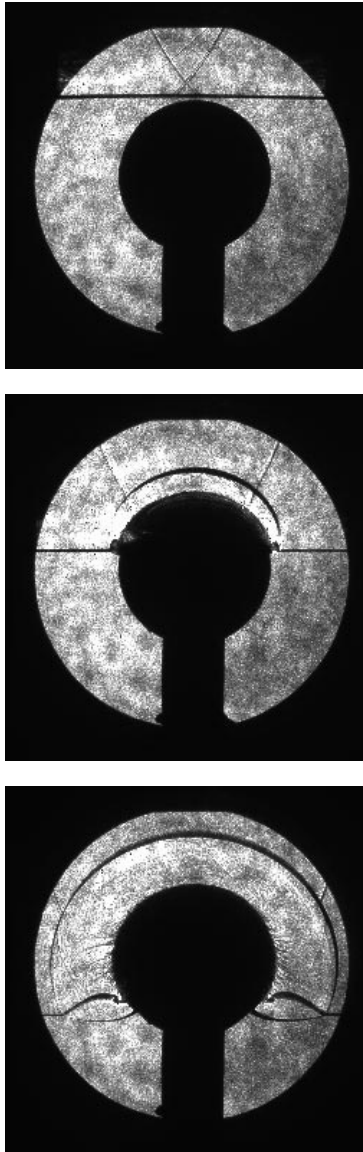


Figure 9. Shadowgraph images of the shock diffraction around a 6.35 cm diameter cylinder at a Mach number of 1.85. The shock was formed from high pressure air into atmospheric air. The successive pictures show the diffraction and reflection of the shock as it contacts the cylinder.

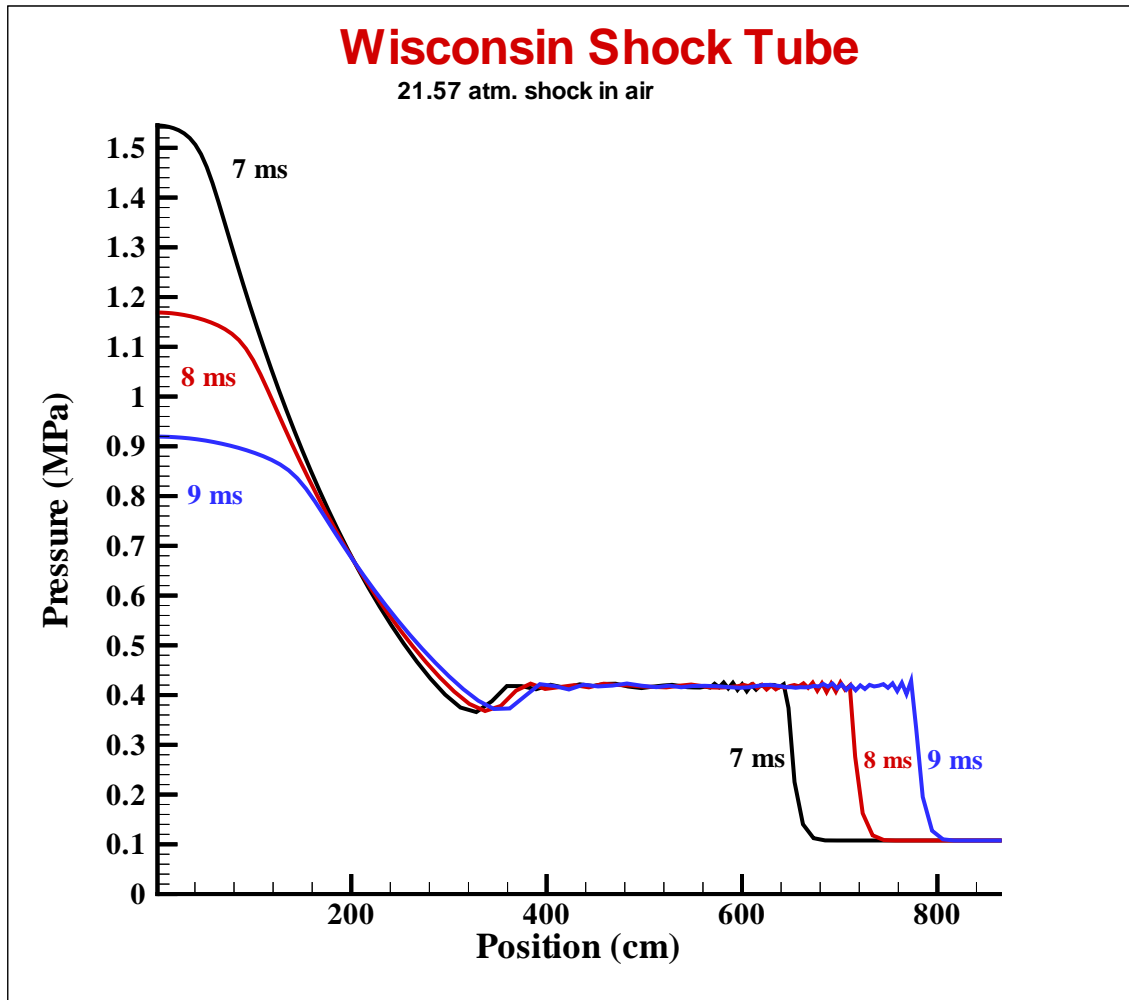


Figure 10. Pressures of shock in Wisconsin Shock Tube. Calculated by BUCKY for $M=1.85$ shock in atmospheric air.

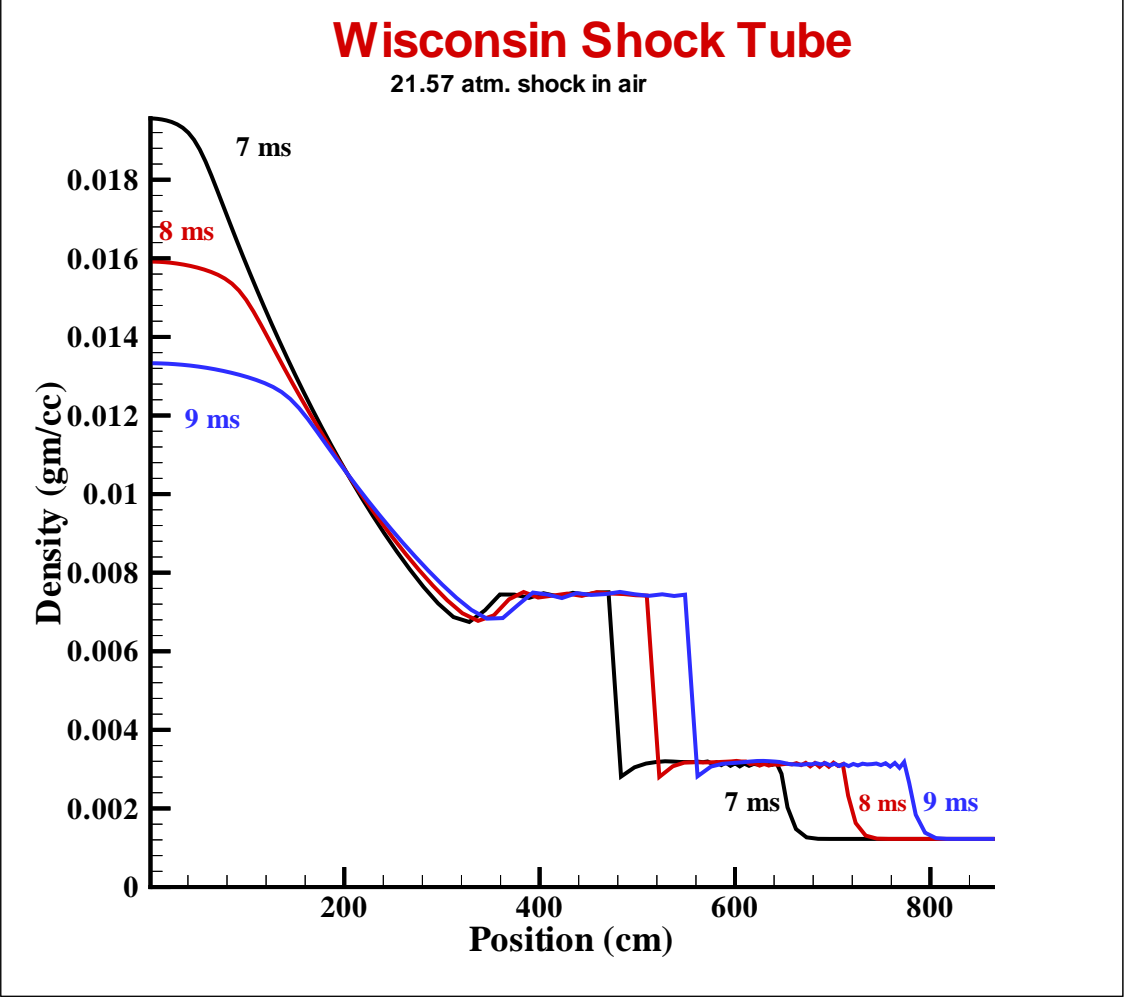


Figure 11. Mass density of shock in Wisconsin Shock Tube. Calculated by BUCKY for $M=1.85$ shock in atmospheric air.

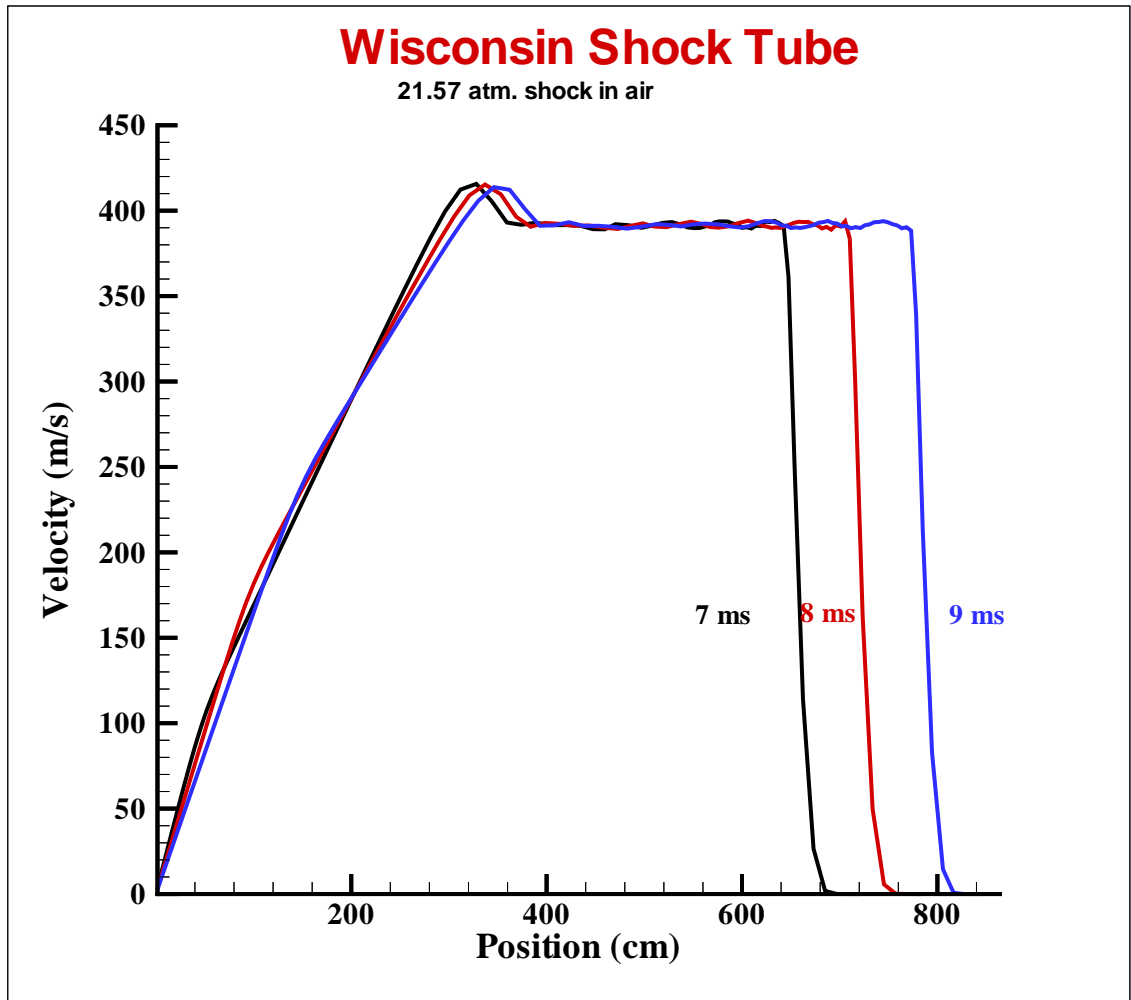


Figure 12. Velocity of shock in Wisconsin Shock Tube. Calculated by BUCKY for $M=1.85$ shock in atmospheric air.



Figure 13. Density of shock in Wisconsin Shock Tube as it flows around a 3.175 cm radius cylinder. Calculated by RAGE for $M=1.85$ shock in atmospheric air.

4. CONCLUSIONS

The physics involved with attaining useful energy from inertial confinement fusion reactions is quite complex and requires experimental investigation. A shock-tube provides an ideal environment to study the hydrodynamic issues related with ICF reactions. The shock-tube has been designed with the purpose of studying these issues in detail and to produce an extension of the existing experimental database into fully compressible flow regimes. Preliminary experiments have been carried out successfully. The results suggest that, in the future, more quantitative data can be obtained using advanced diagnostic techniques that can serve as a set of benchmarking data for numerical codes that simulate hydrodynamic phenomena, such as those described above. These studies will help address issues regarding the cooling tube designs for possible IFE reactors.

Acknowledgment

This work is supported by the U.S. Department of Energy under contract DE-FG02-97ER54413.

REFERENCES

Bennett, B. I., Johnson, J. D., Kerley, G. I., and Rood, G. T., "Recent Developments in the Sesame Equation-of-State Library," Los Alamos National Laboratory Report LA-7130 (February 1978). "T-4 Handbook of Material Properties Data Bases," Los Alamos National Laboratory Report LA-10160-MS (November 1984) K.S. Holian, editor.

Bishop, V. J., Rowe, R. D., The interaction of a long duration friedlander shaped blast wave with an infinitely long right circular cylinder, Atomic Weapons Research Establishment, Aldermaston, Berkshire, England AWRE Report No. 0-38/67 (1967)

Bryson, A. E., Gross, R. F., Diffraction of strong shocks by cones, cylinders, and spheres, Journal of Fluid Mechanics, Vol. 10 part 1, pp. 1-23 (1965)

Heilig, W. H., Diffraction of a shock-wave by a cylinder, Physics of Fluids 12, supplement 1, pt. 2, 154-157 (1969).

Kulcinski G. L., Peterson, R. R., Moses, G. A., et al., Evolution of light ion driven fusion power plants leading to the LIBRA-SP design, Fusion Technology, Vol. 26, pp. 849-856 (1994).

MacFarlane, J. J., Moses, G. A., and Peterson, R. R., "BUCKY-1 – A 1-D Radiation Hydrodynamics Code for Simulating Inertial Confinement Fusion High Energy Density Plasmas," University of Wisconsin Fusion Technology Institute Report UWFD-984 (August 1995).

Meshkov, Y. Y., Instability of liquid surfaces when accelerated in a direction perpendicular to their planes, I, Proc. Roy. Soc. A 201, 192 (1969).

Syshchicova, M. P., Beryozkina, M. K., Semenov, A. N., The flow formation around a body in a shock-tube (in Russian), Collection of papers: the aerophysical investigation of supersonic flows, Science publishers, Moscow, pp. 7-13 (1967).

Wang, P., "EOSOPA – A Code for Computing the Equations of State and Opacities of High-Temperature Plasmas with Detailed Atomic Models," Fusion Power Associates Report FPA-93-8 (December 1993).

Yang, W., Handbook of Flow Visualization, Hemisphere Pub. (1989).